Power sharing between parallel inverters in microgrid by improved droop control

Li Lei
School of Engineering
Newcastle University
Newcastle upon Tyne,
NE1 7RU, UK.
l.lei2@ncl.ac.uk

Mohammed A. Elgendy
School of Engineering
Newcastle University
Newcastle upon Tyne,
NE1 7RU, UK.
mohammed.elgendy@ncl.ac.uk

Neal Wade
School of Engineering
Newcastle University
Newcastle upon Tyne,
NE1 7RU, UK.
neal.wade@ncl.ac.uk

Salaheddine Ethni
School of Engineering
Newcastle University
Newcastle upon Tyne,
NE1 7RU, UK.
salaheddine.ethni@ncl.ac.uk

Hany M. Hasanien
Dept. of Electrical Power and Machines,
Faculty of Engineering
Ain Shams University
Cairo 11517, Egypt.
hanymhasanien@gmail.com

***Abstract*— Microgrid is a main part of the future intelligent and sustainable power system. In order to improve the flexibility of a microgrid and realize the plug and play feature of distributed generation and load, this paper proposed an improved droop control to control the parallel inverters in microgrid to solve the problem that the traditional droop control cannot efficiently allot power between multiple inverters. In the proposed improved droop controller, new components are added to the reference voltage and frequency of each parallel inverter based on a feedback loop of the main bus voltage and frequency, respectively. The proposed control strategy is tested with Matlab/Simulink simulation model of a microgrid in the islanding mode which is more difficult to achieve power sharing in. Different supply and load variations are investigated in order to show the robustness of the proposed control. Results are compared with the traditional droop control showing superior performance of the proposed control.**

Keywords — Distributed generation; Droop control; parallel inverter; Power sharing.

I. Introduction

Energy is the driving force of social and economic development. With the gradual depletion of conventional energy sources and the increasingly prominent ecological and environmental problems, the power industry needs to find a path of sustainable development. With the development of distributed energy, the distribution network has higher requirements for power quality, power supply reliability, and system capacity. Because most of the distributed power in the microgrid needs to be incorporated into the microgrid through inverters, it is important that inverters are controlled in a way that should provide users with high-quality power and increase the reliability of the power distribution system [1-4].

At present, the parallel operation control strategy of the inverter generally adopts master-slave control method [5] and droop control method [6-10]. The master-slave control method requires interconnections for control which limits the distance between distributed power supplies, and introduces noise, so its application has certain limitations [11-12]. The droop control method is an independent control technology without communication signal lines. By using the self-synchronization and voltage droop characteristics of synchronous generators, the parallel operation can be controlled without requiring interconnected signal lines between inverters [13]. It only needs to monitor the output of each inverter and rely on its internal control strategy to achieve synchronization of multiple inverters in parallel and the current sharing operation. Compared with other controls, droop control can make the system simple in structure, complex in function, quick in installation and maintenance, convenient in system expansion, low in cost, and more reliable in parallel operation [14].

With multi-inverter parallel operation, the droop control method is the key technology for inverter control. The reasonable design of its droop coefficient directly affects the dynamic operation of parallel inverters under voltage and frequency variations [15]. The traditional droop control does not perform well in parallel inverter operation, such as it is difficult to achieve rapid power distribution due to the influence of the line parameters, and a large load may cause the system frequency to shift [12]. For equal sharing of linear and nonlinear loads with high accuracy, different improved droop control algorithms have been proposed in [17-19]. The addition of a small signal injection method to improve the reactive power sharing accuracy of a droop controller was also investigated in [20].

Although there are many methods been proposed to achieve equal sharing of linear and nonlinear loads, there still a problem that share loads accurately in proportion to the inverters' power rating [21]. In view of this, this paper proposes a droop-type control method for inverter based distributed generation systems. The output voltage and the bus voltages of the system are measured, and a new compensation amount is included in the droop controller to effectively track the bus voltages variation in the microgrid and efficiently allocate the energy outputs of the parallel inverters. Both the traditional and improved droop control methods are analysed in detail and their performance is compared under the same operating conditions. Matlab/Simulink results show that the proposed droop control has better performance in power sharing compared to the conventional droop control.

978-1-5386-2910-9/18/$31.00 ©2018 IEEE

II. TRADITIONAL DROOP CONTROL

Droop control is based on the relationship between the active power and frequency of the grid-connected inverter and the relationship between its reactive power and voltage, mimicking the droop characteristics of synchronous generator. When used in a microgrid, the inverter power supply voltage and frequency are used as a communication connection with the distribution network, so that there is no physical connection between the distributed units is required to share the load requirements. Conventional droop control can be divided into P-f droop control and P-V droop control as described below.

A. Conventional P-f droop control

The P-f droop control method can be explained by considering a simple microgrid with two parallel inverter-based distributed generation systems operating in parallel (Fig. 1). Inverter output high frequency ripple is filtered out using an LC filter and the output is connect to the AC bus via cables and the relays K_1 and K_2 which control the connection of distributed generation units. r_1 and r_2 are equivalent to the sum of output resistance and line resistance of inverters 1 and 2 while X_1 and X_2 are equivalent to the sum of output reactance and line reactance of inverters 1 and 2, respectively. Z_l is the load impedance. The simplified schematic corresponding to Fig. 1 is shown in Fig. 2 where, $E\angle 0$ is the parallel ac bus voltage, $U_1\angle\varphi_1$ and $U_2\angle\varphi_2$are the no load output voltages of inverters 1 and 2, and φ_1 and φ_2 are the phase angle difference between the no load voltage and the bus voltage of the inverters 1 and 2, respectively.

From Fig. 2, it can be seen that output active power and reactive power of inverter i (i=1, 2) are:

$$P_i = \frac{1}{|Z_i|}[(EU_i cos\varphi_i - E^2)cos\theta_i + EU_i sin\varphi_i sin\theta_i] \quad (1)$$

$$Q_i = \frac{1}{|Z_i|}[(EU_i cos\varphi_i - E^2)sin\theta_i - EU_i sin\varphi_i cos\theta_i] \quad (2)$$

where $|Z_i|$ is the corresponding impedance amplitude of inverter i:

$$|Z_i| = \sqrt{r_i^2 + X_i^2} \quad (3)$$

$$\theta_i = arctan\frac{r_i}{X_i} \quad (4)$$

Normally, φ_i is small and can be approximated as $\sin\varphi_i = \varphi_i$, $\cos\varphi_i = 1$. When X_i is much larger than r_i, euqations (1) and (2) can be written as:

$$P_i \approx \frac{EU_i}{X_i}\varphi_i \quad (5)$$

$$Q_i \approx \frac{E}{X_i}(U_i - E) \quad (6)$$

It can be seen from the above equation that the active output power of the inverter is mainly affected by the phase angle difference between the no-load output voltage of the inverter and the bus, while the reactive power output of the inverter is mainly affected by the output voltage amplitude of the no load output of the inverter. Because of the phase angle difference between the no load output voltage of the inverter and the bus bar is difficult to detect, the frequency is generally used instead in inverter control. The P-f control equations can be expressed as:

$$f_i = f_{0i} - m_i(P_i - P_{0i}) \quad (7)$$

$$U_i = U_{0i} - n_i(Q_i - Q_{0i}) \quad (8)$$

where f_i and U_i are output frequency and output voltage of inverter, respectively; f_{0i} and U_{0i} are rated frequency and rated voltage of inverter, respectively; m_i and n_i are inverter droop coefficient of P/f and Q/U, respectively; P_i and Q_i are active power and reactive power of inverter, respectively; P_{0i} and Q_{0i} are rated active power and rated reactive power of inverter, respectively.

The advantages of the P-f droop control are avoiding critical communication link, great flexibility and high reliability. The disadvantages are slow dynamic response, poor harmonic load sharing, line impedance mismatch affects power sharing, and poor performance with renewable energy resources.

B. Conventional P-V droop control

P-V droop control, also known as anti-droop control, in the actual low voltage microgrid, the line impedance is resistive mainly, r_i is much bigger than X_i, the sum of inverter output inductances and line inductances can be neglected. Meanwhile, the phase angle φ_i is very small, so that $\sin\varphi_i = \varphi_i$, $\cos\varphi_i = 1$, then:

$$P_i \approx \frac{U_i(U_i - E)}{R_i} \quad (9)$$

$$Q_i \approx -\frac{U_i\theta_i E}{R_i} \quad (10)$$

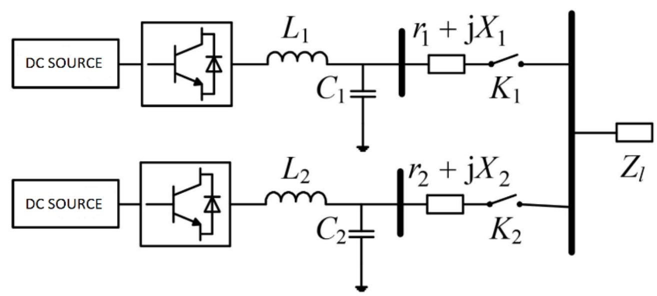

Fig.1 Structure of a microgrid with two distributed generations.

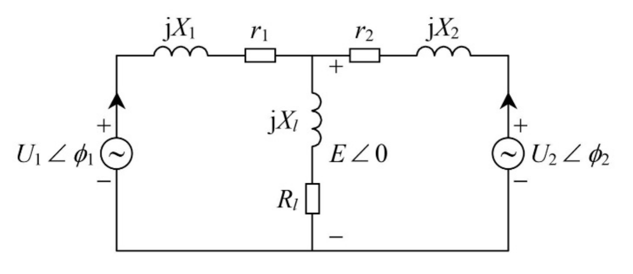

Fig.2 Schematic diagram of a microgrid with two distributed generations.

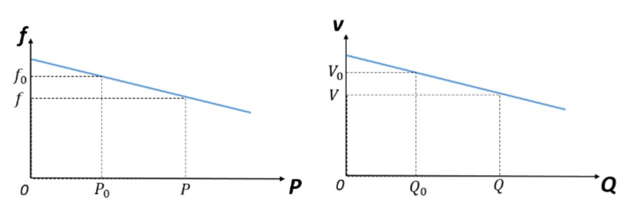

Fig.3 Droop characteristic of P-f droop control.

From the above equation, the inverter output active power of the inverter is mainly affected by the inverter no-load output voltage amplitude, and the inverter output reactive power is mainly affected by the phase angle difference between the inverter no-load output voltage and the bus. Similar to the P-f droop control, the frequency is used in inverter control instead of the phase angle, and the P-V droop control can be shown as:

$$f_i = f_{0i} - u_i(Q_i - Q_{0i}) \tag{11}$$

$$U_i = U_{0i} - v_i(P_i - P_{0i}) \tag{12}$$

where u and v are droop coefficient and the other parameters are same as P-f droop control.

From the above analysis of the characteristics of the high voltage and low voltage line impedance, when the active and reactive power output from the inverter deviates from the rated active and reactive power, the voltage and frequency values also have a certain amount of deviation from the rated value.

C. Power sharing of conventional droop control.

Fig. 5 shows a block diagram of two inverters operating in parallel with traditional droop control based on resistive lines. According to equations 11 and 12, when the frequency of two inverters equals ($f_1 = f_2$), the system is stable. In this case, when the droop coefficient is inversely proportional to its rated power as in (13), inverter output reactive power will be distributed based on droop coefficients (15).

$$f_{01} = f_{02} \tag{13}$$

$$u_1 Q_{01} = u_2 Q_{02} \tag{14}$$

$$u_1 Q_1 = u_2 Q_2 \tag{15}$$

Substitute the value of Q from (10), we get:

$$u_1 \frac{EU_1}{R_1}\theta_1 = u_2 \frac{EU_2}{R_2}\theta_2 \tag{16}$$

If $\theta_1 = \theta_2$ and $U_1 = U_2$, then:

$$\frac{u_1}{R_1} = \frac{u_2}{R_2} \tag{17}$$

For active power, based on (12), to achieve equal power sharing, the conditions in (18) and (19) should be satisfied:

$$U_{01} = U_{02} \tag{18}$$

$$v_1 P_{01} = v_2 P_{02} \tag{19}$$

When $U_1 = U_2$,

$$v_1 P_1 = v_2 P_2 \tag{20}$$

Substitute (9) into (20), we can get:

$$v_1 \frac{U_1(U_1 - E)}{R_1} = v_2 \frac{U_2(U_2 - E)}{R_2} \tag{21}$$

Then, with $U_1 = U_2$, we get:

$$\frac{v_1}{R_1} = \frac{v_2}{R_2} \tag{22}$$

The inverter output active power will equally distributed following rated value.

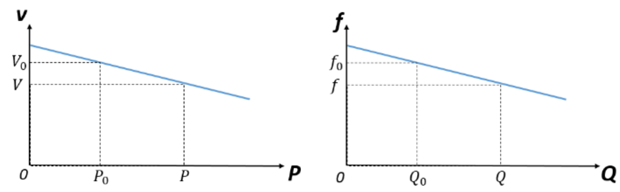

Fig.4 Droop characteristic of P-V droop control.

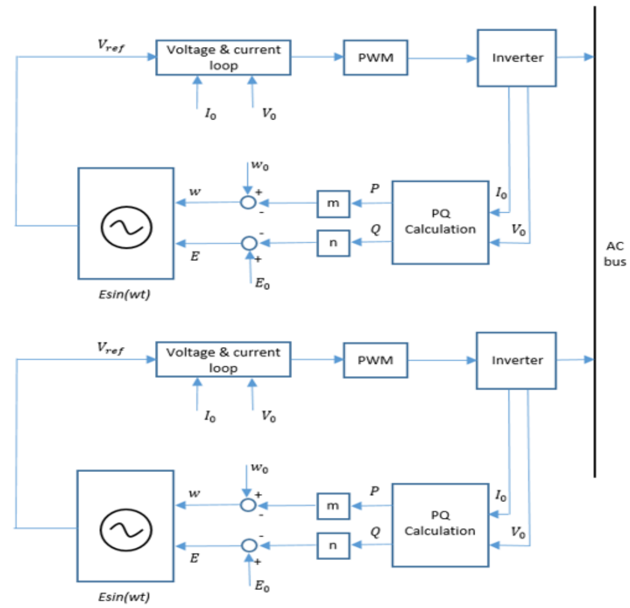

Fig.5 Two inverters operation in parallel.

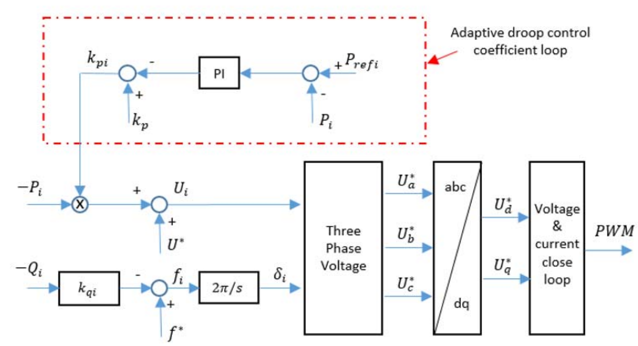

Fig.6 Block diagram of adaptive regulating droop coefficient control for DG.

III. IMPROVED DROOP CONTROL

A. Adaptive P-V droop control

Fig. 6 shows the block diagram of an adaptive P-V droop control proposed in [12]. The outer loop is to control the output power to respond to load variations. The voltage and current double inner loops are responsible for stabilizing the output voltage and improving the dynamic response of the current. In this method, the active droop coefficient is automatically adjusted according to the output power. The droop control equations are:

$$U_i = U_i^* - [k_p - (D_p + D_i/s)(P_{refi} - P_i)]P_i \quad (23)$$

$$f_i = f_i^* + k_{qi}Q_i \quad (24)$$

where k_p is rated active droop coefficient; D_p and D_i are the proportional and integral coefficients of the PI regulator of the power control loop, respectively; P_{refi} is rated active power of DGi. This adaptive droop control method can be used with parallel inverters by dividing the active power equally between n units DG in island mode, as in (25):

$$P_{refi} = (P_1 + P_2 + \cdots + P_n)/n \quad (25)$$

To distribute the load proportionally, P_{refi} is calculated by a central controller and sent to the local controller of the inverter.

Fig. 7 shows how the droop curve is adjusted automatically. At the beginning, the two inverters use the same drooping coefficient k_p. Since the line impedance does not coincide with $m_{p2} > m_{p1}$, the active power of DG_2 will be lower than that of DG_1. As the output power of each inverter deviates from $P_{ref} = (P_1 + P_2)/2$, then the droop coefficients need to be adjusted in order to follow the reference power. For DG_1, the inverter output power $P_1 > P_{ref}$, so the PI controller output is negative and because k_p is positive, the DG_1 droop coefficient gradually increases to k_{p1}, at which $P_1 = P_{ref}$. Similarly, for DG_2, the droop coefficient decreases from k_p to k_{p2} to achieve $P_2 = P_{ref}$ and therefore accurate equalization of active power with DG_1.

B. *Proposed improved adaptive droop control*

The improved droop control method proposed in this paper is similar to the above discussed adaptive droop control method in terms of adding an outer control loop for power to the traditional droop control. However, with the proposed method the outer loop adjustment is for inverter's voltage and frequency and it focuses more on power sharing between parallel inverters. The bus side voltage value is fed back to the droop control loop, so that the system can accurately track the load and the generation variations. The changes make the power output of parallel inverters more accurate and enhance the dynamic response of the system.

Fig. 8 shows the block diagram of the proposed improved droop control. The added outer loop control is encircled in red. U_{bus} is the main voltage value, and f_{bus} is the main bus frequency.

Therefore, for improved droop control, the output voltage and frequency calculation formulas are:

$$\omega_o = 2\pi \times [(P_{ref} - P) \times m + f_n + \delta_f] \quad (26)$$

$$U_o = (Q_{ref} - Q) \times n + U_n + \delta_E \quad (27)$$

where δ_f and δ_E are the outer loop frequency and voltage values that are fed back to the droop control.

IV. SIMULATION RESULTS

To verify the effectiveness of the proposed droop control method, this part mainly focuses on the simulation results of the entire system performed using Matlab/Simulink. To verify that improved droop control has superior performance over the traditional droop control, performance is compared based on three measurement parameters. The first is main bus frequency which is analyzed under load and generation changes. The second is the output power for each individual inverter and the third is the voltage of the main bus.

The simulated system topology is shown in Fig. 9. As shown, there are two distributed generation system. They both have inverter and system parameters are listed in Table I. DG_1 straight connected to load, there is a three phase breaker between DG_2 and load. Model have two loads and is connected to grid. Load 1 has 2000W active power and 600W inductive reactive power while load 2 has 2000W active power and 0W reactive power. The grid phase-to-phase voltage is 380V. Table II depicts the operation mode based on the state of the two breakers.

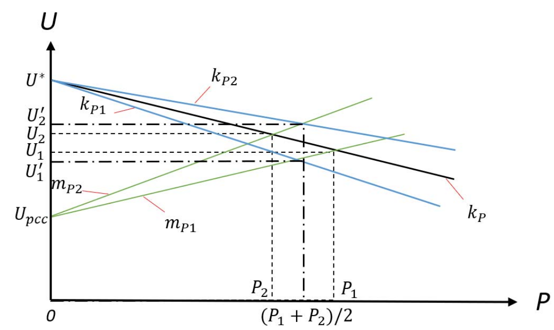

Fig.7 Adaptive regulating of P-V droop coefficient.

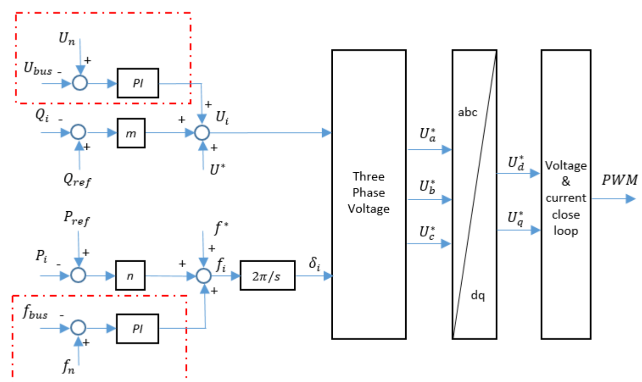

Fig.8 Improved droop control method.

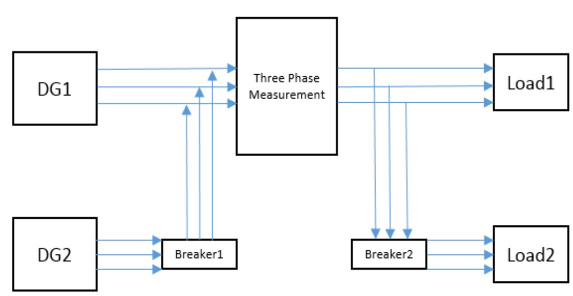

Fig.9 Simulation system topology.

TABLE I. PARAMETER OF THE SYSTEM

	Parameters	Value
Power parameters	Inverter switching frequency	10kHz
	DC bus voltage	800V
	Nominal bus frequency	50Hz
	RMS line voltage	380V
	Filter inverter-side inductance(DG1)	3mH, 0.2Ω
	Filter inverter-side inductance(DG2)	6mH, 0.4Ω
	Filter grid-side inductance	0.264mH, 0.642Ω
	Filter capacitor	150μF
Controller parameters	Droop control	
	Frequency droop coefficient **m**	1e-5
	Voltage droop coefficient **n**	2e-4
	Voltage control	
	Transfer function **num(s)/den(s)**	[0.2 280.8]/[1 0]
	Current control	
	Proportional term **Kp**	0.24

TABLE II. OPERATION MODE

Breaker number	Time	Operation
1	0.5 s	DG 2 connect to the bus.
2	5.0 s	Load 2 connect to the bus.

From Table 2, it can be seen that there are two time points in this model. At 0.5 s, DG_2 is connected to the bus. At 5 s, Load 2 is connected to the bus. This allows testing of the considered control methods under load and generation variations.

Fig. 10 and Fig. 11 show the frequency response of the traditional and improved droop control, respectively. It can be seen that the frequency of improved droop control has lower steady-state oscillations at slightly higher transient overshoot. Figures 12-15, show that the output active power of improved droop control is more accurate distributed between the two generators. When DG_2 is connected, the load is equally distributed between the two generators, unlike the case with the traditional droop control. Similarly, when the Load 2 is connected, the active power shares are adjusted better with the proposed droop control method. The improved droop control method offers also lower steady-state oscillations. Fig. 16 and Fig. 17 show the main bus voltage with the conventional and improved droop control methods. As illustrated, the proposed droop control method has better voltage regulation for the main bus voltage. On the other hand, with the conventional droop control, the voltage of the main bus decreases with load increase.

The simulation results discussed above clearly show that, for the same system parameters, the improved droop control has a strong advantage over the traditional droop control in terms of power distribution and voltage and frequency stability. Therefore, it can be a strong candidate for power sharing control of the parallel inverter operation in microgrids.

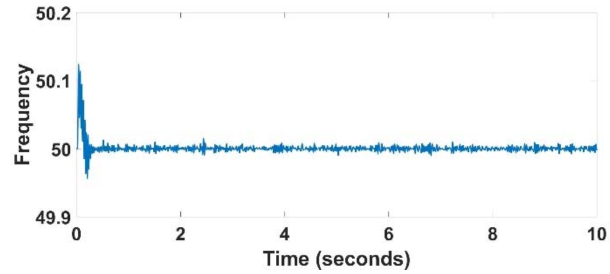

Fig.10 Main bus frequency of traditional droop control.

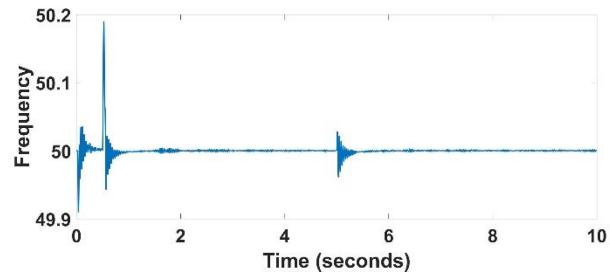

Fig.11 Main bus frequency of improved droop control.

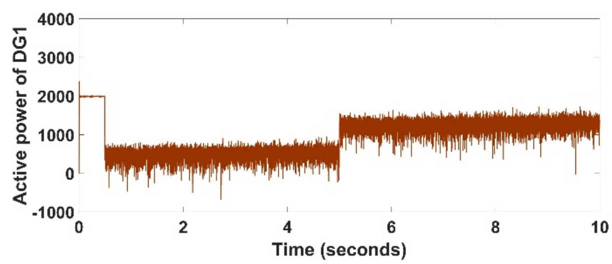

Fig. 12 Active power of DG1 for traditional droop control.

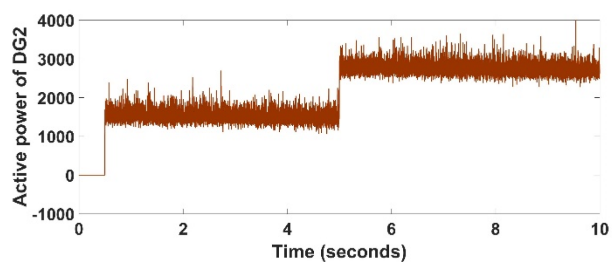

Fig. 13 Active power of DG2 for traditional droop control.

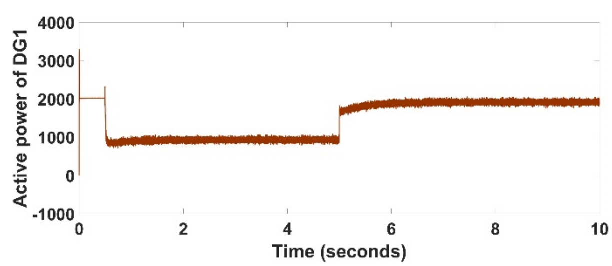

Fig.14 Active power of DG1 for improved droop control.

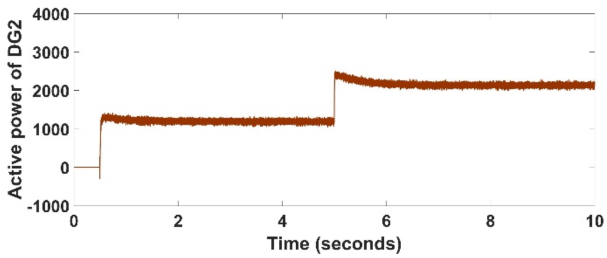

Fig.15 Active power of DG2 for improved droop control.

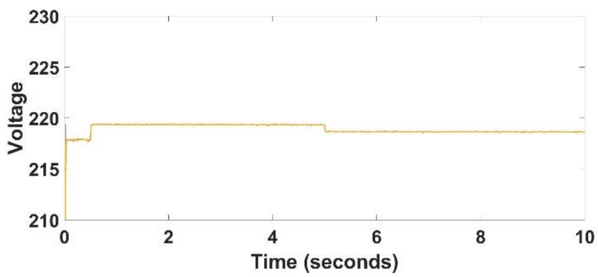

Fig.16 Output voltage of traditional droop control.

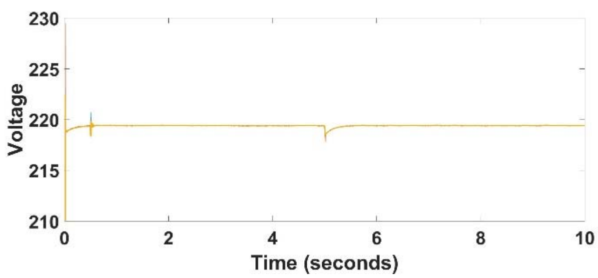

Fig.17 Output voltage of improved droop control.

V. CONCLUSION

This paper proposed an improved droop control method that can better suit parallel operation of inverter based distributed generation systems. Firstly, the traditional droop control methods were discussed and their drawback in parallel operation of converters is highlighted. An adaptive droop control method is then discussed and the same concept is used in the proposed control method. Simulation model was constructed to analyze the performance of the improved droop control and to compare it to the traditional droop control. Results show that the improved droop control method has superior performance in terms of load sharing and voltage and frequency regulation compared to the conventional droop control method. In the future, the simulation results will be experimentally validated using the hardware in the loop and converter facilities at Newcastle University.

REFERENCES

[1] W. Zhang, M. Armstrong and M. A. Elgendy, "DC component detection in grid connected inverter systems, using a mid-ground low pass filter approach", IET International Conference on Power Electronics, Machines and Drives PEMD 2016, Glasgow, UK, 19 – 21 April 2016.

[2] A. Althobaiti, M. Armstrong and M. A. Elgendy, "Current control of three-phase grid-connected PV inverters using adaptive PR controller", IEEE International Renewable Energy Congress IREC 2016, Hammamet, Tunisia, 21-23 March 2016.

[3] A. Althobaiti, M. Armstrong and M. A. Elgendy, "Control parameter optimization of a three phase grid connected inverter using Particle Swarm Optimisation", IET International Conference on Power Electronics, Machines and Drives PEMD 2016, Glasgow, UK, 19 – 21 April 2016.

[4] M. A. Elgendy, D. J. Atkinson, M. Armstrong, S. M. Gadoue "Impact of grid background harmonics on inverter-based islanding detection algorithms", IEEE International Conference on Power Electronics and Drive Systems PEDS 2015, Sydney, Australia, 9-12 June 2015.

[5] J. P. Lopes, C. L. Moreira and A. G. Madureira, "Defining control strategies for microgrids islanded operation," IEEE Trans. Power Systems, vol. 21, no. 3, pp. 916-924, 2006.

[6] J. M. Guerrero, L. Hang and J. Uceda, "Control of distributed uninterruptible power supply systems," IEEE Trans. Industrial Electronics, vol. 55, no. 8, pp. 2845-2859, 2008.

[7] E. A. A. Coelho, P. C. Cortizo and P. F. D. Garcia, "Small-signal stability for parallel-connected inverters in stand-alone AC supply systems," IEEE Trans. Industry Applications, vol. 38, no. 2, pp. 533-542, 2002.

[8] X. Sun, Y. S. Lee and D. Xu, "Modeling, analysis, and implementation of parallel multi-inverter systems with instantaneous average-current-sharing scheme," IEEE Trans. Power Electronics, vol. 18, no. 3, pp. 844-856, 2003.

[9] J. M. Guerrero, L. G. De Vicuña, J. Matas, M. Castilla and J. Miret, "Output impedance design of parallel-connected UPS inverters with wireless load-sharing control," IEEE Trans. Industrial Electronics, vol. 52, no. 4, pp. 1126-1135, 2005.

[10] E. Barklund, N. Pogaku, M. Prodanovic, C. Hernandez-Aramburo and T.C. Green, "Energy management in autonomous microgrid using stability-constrained droop control of inverters," IEEE Trans. Power Electronics, vol. 23, no. 5, pp. 2346-2352, 2008.

[11] T. Fang, X. Ruan, L. Xiao and A. Liu, (2008, June) "An improved distributed control strategy for parallel inverters," IEEE Power Electronics Specialists Conference (PESC), pp. 3500-3505, Jun. 2008.

[12] L. Xiao, A. Z. Liu, T. Z. Fang and X. B. Ruan, "Multi-inverter parallel system applying average current controlling method," PROCEEDINGS-CHINESE SOCIETY OF ELECTRICAL ENGINEERING, vol. 28, no. 3, pp. 77, 2008.

[13] A. Tuladhar, H. Jin, T. Unger and K. Mauch, "Parallel operation of single phase inverter modules with no control interconnections," IEEE Applied Power Electronics Conference and Exposition, 1997 APEC'97, vol. 1, pp. 94-100, Feb. 1997.

[14] Z. Yao, M. Hao, L. Biao and H. Xiangning, "Analysis of dynamic performance for parallel operation of inverters without wire interconnections," Proceedings of the CSEE, vol. 29, no. 3, pp.42-48, 2009.

[15] J. M. Guerrero, L. G. De Vicuña, J. Matas, M. Castilla and J. Miret, "Output impedance design of parallel-connected UPS inverters with wireless load-sharing control," IEEE Trans. Industrial Electronics, vol. 52, no. 4, pp. 1126-1335, 2005.

[16] J. Li, F. Li, X. Li, H. Liu, F. Chen and B. Liu, "S-shaped droop control method with secondary frequency characteristics for inverters in microgrid," IET Generation, Transmission & Distribution, vol. 10, no. 13, pp. 3385-3392, 2016.

[17] J. M. Guerrero, L. G. De Vicuña, J. Matas, M. Castilla and J. Miret, "Output impedance design of parallel-connected UPS inverters with wireless load-sharing control," IEEE Trans. Industrial Electronics, vol. 52, no. 4, pp. 1126-1135, 2005.

[18] J. M. Guerrero, J. Matas, L. G. De Vicuna, M. Castilla and J. Miret, "Decentralized control for parallel operation of distributed generation inverters using resistive output impedance," IEEE Trans. Industrial Electronics, vol. 54, no. 2, pp. 994-1004, 2007.

[19] U. Borup, F. Blaabjerg and P. N. Enjeti, "Sharing of nonlinear load in parallel-connected three-phase converters," IEEE Trans. Industry Applications, vol. 37, no. 6, pp. 1817-1823, 2001.

[20] A. Tuladhar, H. Jin, T. Unger and K. Mauch, "Control of parallel inverters in distributed AC power systems with consideration of line impedance effect," IEEE Trans. Ind. Appl., vol. 36, no. 1, pp. 131-138, 2000.

[21] Y. W. Li and C. N. Kao, "An accurate power control strategy for power-electronics-interfaced distributed generation units operating in a low-voltage multibus microgrid," IEEE Trans. Power Electronics, vol. 24, no. 12, pp. 2977-2988, 2009.

[22] N. R. Chaudhuri and B. Chaudhuri, "Adaptive droop control for effective power sharing in multi-terminal DC (MTDC) grids," IEEE Trans. Power Systems, vol. 28, no. 1, pp. 21-29, 2013.